Colloid Polym Sci (2007) 285:1543–1552
DOI 10.1007/s00396-007-1721-x

ORIGINAL CONTRIBUTION

Dissipative particle dynamics simulation of gold nanoparticles stabilization by PEO–PPO–PEO block copolymer micelles

Shu Chen · Chen Guo · Guo-Hua Hu · Hui-Zhou Liu · Xiang-Feng Liang · Jing Wang · Jun-He Ma · Lily Zheng

Received: 14 January 2007 / Revised: 24 May 2007 / Accepted: 13 June 2007 / Published online: 14 July 2007

Abstract Dissipative particle dynamics (DPD) was used to simulate the formation and stabilization of gold nanoparticles in poly(ethylene oxide)–poly(propylene oxide)–poly(ethylene oxide) (PEO–PPO–PEO) block copolymer micelles. Primary gold clusters that were experimentally observed in the early stage of gold nanoparticle formation were modeled as gold bead in DPD simulation. It showed that gold beads were wrapped by the block copolymer and aggregated into spherical particles inside the micelles and forming stable Pluronic–gold colloids with two-layer structures. Increasing Pluronic concentration, molecular weight, and PPO block length led to the formation of more uniform and more stable gold nanoparticles. Density profiles of water beads suggested that the micelles, especially the hydrophobicity of the micellar cores, played an important role in stabilizing gold nanoparticles. Dynamic process indicated that the formation of gold nanoparticles was controlled by the competition between aggregation of primary gold clusters and the stabilization by micelles of block copolymers.. The DPD simulation results of gold–copolymer–water system agree well with previous experiments, while more structure information on microscopic level could be provided.

Keywords Dissipative particle dynamics · Block copolymer · Micelle · Nanoparticle · Stabilization

S. Chen · C. Guo (✉) · H.-Z. Liu (✉) · X.-F. Liang · J. Wang · J.-H. Ma · L. Zheng
Laboratory of Separation Science and Engineering,
State Key Laboratory of Biochemical Engineering,
Institute of Process Engineering, Chinese Academy of Sciences,
Beijing 100080, China
e-mail: cguo@home.ipe.ac.cn
e-mail: hzliu@home.ipe.ac.cn

S. Chen
e-mail: chenshu@home.ipe.ac.cn

S. Chen · C. Guo · H.-Z. Liu · X.-F. Liang · J. Wang · J.-H. Ma · L. Zheng
Graduate School of the Chinese Academy of Sciences,
Beijing 100049, China

G.-H. Hu
Laboratory of Chemical Engineering Sciences,
CNRS-ENSIC-INPL,
1 rue Grandville, BP 20451,
54001 Nancy Cedex, France

G.-H. Hu
Institut Universitaire de France, Maison des Universités,
103 Boulevard Saint-Michel,
75005 Paris, France

Introduction

Nanoparticles are often fairly unstable in solutions. Thus, stabilization is crucial to prevent them from aggregation and to finely control their size and shape. A strategy consists in using amphiphilic micelles or reversed micelles as stabilizers, which confers distinct advantages in controlling the dispersed particles due to good tunability of the templates with variation of the amphiphilic characteristics and the solvent quality [1]. Recently, Sakai and Alexandridis [2] reported that poly(ethylene oxide)–poly(propylene oxide)–poly(ethylene oxide) (PEO–PPO–PEO) block copolymer (Pluronic) was very efficient on stabilization of gold nanoparticles. That novel procedure was simple, environmentally benign, and economic. In our previous work, we present controlling gold nanoparticles stabilization by tuning hydrophobic properties inside PEO–PPO–PEO block copolymer micelles [3]. By modulating the concentration and compo-

sition of PEO–PPO–PEO block copolymer and adding NaF salt as additives, gold nanoparticles with different sizes and morphologies could be obtained.

Although amphiphilic micelles/reverse micelles were widely employed as nanoparticle stabilizers, the role of their micro-level properties on controlling the growth and formation of nanoparticles was still ambiguous and rarely reported. Investigations on the microenvironments and microstructures of micelles in nanoparticle–amphiphilic polymer assemblies might shed light on this important issue [4, 5]. It would also give some guidance on the discovery of novel materials. For example, the conformational behavior of the polymer and the distributions of elements inside the composites will be helpful for disclosing the mechanism of their formation and stabilization. Knowledge of the dynamics during the formation process not only allows an understanding of the formed structures but will also enable one to control the morphology of the prepared structures. However, it is not easy to probe the detailed information on microscopic level and dynamic process experimentally.

Computational simulation may be helpful to tackle the problems mentioned above. Dissipative particle dynamics (DPD) simulation, a mesoscopic method developed by Hoogerbrugge and Koelman [6], appears to be suitable for simulating systems that contain millions of atoms in nanosecond time and nanometer length scales [7, 8]. In DPD, one treat simulated elements in a coarse-grained level by grouping atoms together up to a single bead. The beads feel a simple soft pair-wise interaction potential that allows large time-scale simulations. Time evolution of the system is found by solving Newton's equations of motion. In the past decade, DPD method has been applied to numerous complex systems such as biological membranes [9–13], polymeric vesicles [14–19], self assembly of amphiphilics [20–26], and interfacial phenomena [27–30]. Recently, this method allowed successfully reproducing the micellization of PEO–PPO–PEO block copolymers [31]. It also proved effective to investigate several types of nanocomposites [32, 33], especially the growth of gold nanoparticles in the presence of thiol-terminated oligohydroquinonyl ether as stabilizer [34].

To explore new insights into the relationship between properties of micelles and nanoparticles stabilized by them, simulations on gold nanoparticles stabilized by PEO–PPO–PEO block copolymer micelles as a model system is necessary. In this study, we adopted DPD to simulate this complex system composed of Au atoms, PEO–PPO–PEO block copolymer, and water. Primary gold clusters that were experimentally observed in the early stage of gold nanoparticles formation were modeled as gold bead [3], allowing specific physical origin of gold bead in simulation. The effect of block copolymer concentration and composition on the stabilization of gold nanoparticles was investigated. The density distribution of water beads was calculated to measure the hydrophobicity inside the Pluronic–gold colloids. All simulation results demonstrated that DPD methods are effective to study the nanoparticle–polymer systems.

Simulation method

Theory The DPD model used in this work is based on that of Groot and Warren [7, 8]. Molecules are divided into soft beads. The evolution of the positions and impulses of all interacting beads over time is governed by Newton's equations:

$$\frac{\mathrm{d}\vec{r}_i}{\mathrm{d}t} = \vec{v}_i, \frac{\mathrm{d}\vec{v}_i}{\mathrm{d}t} = \vec{f}_i \tag{1}$$

where $\vec{r}_i$, $\vec{r}_i$, and $\vec{f}_i$ are the position vector, velocity, and total force on the ith bead, respectively. The total force exerted on bead i contains three parts, each of which is pair-wise additive.

$$F_i = \sum_{i \neq j} \left(F_{ij}^{\mathrm{C}} + F_{ij}^{\mathrm{D}} + F_{ij}^{\mathrm{R}} \right) \tag{2}$$

where F_{ij}^{C} is the conservative force and is linear in the bead–bead separation; F_{ij}^{D} is the dissipative force and is proportional to the relative velocity of beads i and j; and F_{ij}^{R} is the random force between bead i and its neighboring bead j. They are given, respectively, by

$$F_{ij}^{\mathrm{C}} = a_{ij}\omega(r_{ij})\hat{r}_{ij} \tag{3}$$

$$F_{ij}^{\mathrm{D}} = -\gamma\omega^{\mathrm{D}}(r_{ij})(\hat{r}_{ij} \cdot v_{ij})\hat{r}_{ij} \tag{4}$$

$$F_{ij}^{\mathrm{R}} = \sigma(\Delta t)^{-1/2}\omega^{R}(r_{ij})\theta_{ij}\hat{r}_{ij} \tag{5}$$

where $\vec{r}_{ij} = \vec{r}_i - \vec{r}_j$, $\vec{v}_{ij} = \vec{v}_i - \vec{v}_j$, $r_{ij} = |\vec{r}_{ij}|$, and $\hat{r}_{ij} = \vec{r}_{ij} / r_{ij}$. Beads interact only with those that are within a certain cut-off radius r_c. The weight factor $\omega(r)$ determines the details of the conservative force. It is normally $\omega(r)=1-r/r_c$ for $r \leq r_c$ and $\omega(r)=0$ for $r>r_c \cdot a_{ij}$ is a maximum repulsive parameter between beads i and j and is referred to as bead–bead repulsion parameter. It depends on the underlying atomistic interactions. Unlike the conservative force, the weight functions ω^{D} (r) and ω^{R} (r) of the dissipative forces and random forces couple together to form a thermostat. Espanol and Warren showed that the system relaxes to a Gibbs–Boltzmann equilibrium distribution when the correct thermostat is applied [7]. They proved that this holds true if the random and dissipative forces are

balanced and related to the system temperature according the fluctuation-dissipation theorem.

$$\omega^{\mathrm{D}}(r) = \left[\omega^{\mathrm{R}}(r)\right]^2 \tag{6}$$

$$\sigma^2 = 2\gamma k_{\mathrm{B}} T \tag{7}$$

where γ and σ are the two multiplicative constants that are related by absolute temperature T, and k_{B} is the Boltzmann constant. The weight functions can have the following simple form $\omega^{\mathrm{D}}(r) = [\omega^{\mathrm{R}}(r)]^2 = (1 - r/r_c)^2$, for $r \leq r_c$.

θ_{ij} is a symmetric random variable satisfying the following two conditions:

$$\langle \theta_{ij}(t) \rangle = 0 \tag{8}$$

$$\langle \theta_{ij}(t)\theta_{kl}(t') \rangle = \left(\delta_{ik}\delta_{jl} + \delta_{il}\delta_{jk}\right)\delta(t - t') \tag{9}$$

where, $i \neq j$ and $k \neq l \cdot \Delta t$ is the iteration time step.

Finally, the soft particles in a polymer chain are connecting one by one via the harmonic springs with a spring force $F_{ij}^{\mathrm{S}} = C\bar{r}_{ij}$, where C is the spring constant. Newton's equations of positions and velocities of particles are solved by a modified version of the velocity-Verlet algorithm [7, 8]. Random initial configurations are created by assigning random position coordinates to all beads, subject to the constraint that adjacent beads in a polymer chain are not separated by more than a bead diameter to prevent artificially large forces occurring in the initial state. The dynamic behaviors of beads are followed along trajectories through the phase space by integrating the equations of motions. The simulations in this paper are performed with $k_{\mathrm{B}}T$=1.0, σ=3.0, γ=4.5, Δt=0.05, and C=4.0.

In DPD simulations, the bead mass and radius (actually the range of bead–bead interactions) have been set equal to unity. The time unit is specified as $\sqrt{\left(mr_c^2/k_{\mathrm{B}}T\right)}$ according to the theorem of equipartition of energy. Hence, all the quantities in a DPD simulation are dimensionless. To relate the results of a simulation to a real system, the bead positions, velocities, and distributions can be converted into physical units by scaling with the appropriate combinations of these three fundamental values. If the triplet (r, v, t) represents a length, velocity, and time in physical units, the corresponding quantities in the DPD simulation are given by:

$$\bar{r} = \frac{r}{r_c}, \bar{v} = \frac{v}{\sqrt{k_{\mathrm{B}}\frac{T}{m}}}, \bar{t} = \frac{t}{\sqrt{\frac{mr_c^2}{k_{\mathrm{B}}T}}} \tag{10}$$

Using these conversions formulate that it is possible to extract quantitative results from DPD calculation such as diffusion coefficients, interfacial tension, and so on.

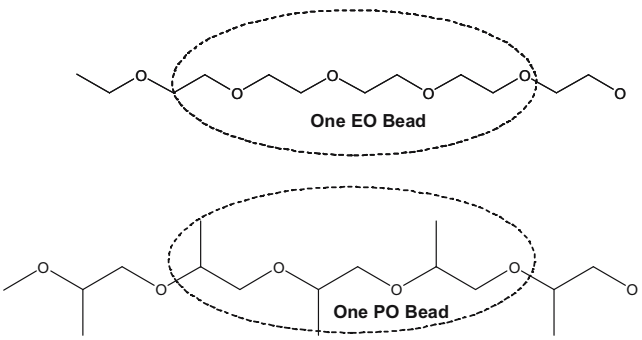

Fig. 1 Schematic representation of block copolymer in DPD system

Table 1 Nominal formula and coarse-gained chains of the Pluronic polymers used in this study

Pluronic	Nominal formula	Coarse-grained chains
F108	$(EO)_{132}(PO)_{51}(EO)_{132}$	$(E)_{33}(P)_{17}(E)_{33}$
F88	$(EO)_{104}(PO)_{39}(EO)_{104}$	$(E)_{26}(P)_{13}(E)_{26}$
F68	$(EO)_{76}(PO)_{30}(EO)_{76}$	$(E)_{19}(P)_{10}(E)_{19}$
F38	$(EO)_{44}(PO)_{18}(EO)_{44}$	$(E)_{11}(P)_{6}(E)_{11}$
P105	$(EO)_{36}(PO)_{54}(EO)_{36}$	$(E)_{9}(P)_{18}(E)_{9}$
P123	$(EO)_{20}(PO)_{69}(EO)_{20}$	$(E)_{5}(P)_{23}(E)_{5}$
P84	$(EO)_{20}(PO)_{42}(EO)_{20}$	$(E)_{5}(P)_{14}(E)_{5}$
P65	$(EO)_{20}(PO)_{30}(EO)_{20}$	$(E)_{5}(P)_{10}(E)_{5}$
PEO	$(EO)_{40}$	$(E)_{10}$

Simulation system and parameters The system that is simulated in this work is composed of water, PEO–PPO–PEO block copolymer, and gold atoms. The PEO–PPO–PEO block copolymer is treated as a coarse-grained chain. Four EO segments are a DPD bead, so as for three PO segments (Fig. 1). This way of mapping a PEO–PPO–PEO block copolymer is similar to the Gaussian chain description used in Mesodyn (another important mesoscale simulation method) [35, 36]. According to previous studies on the partial volumes of EO groups and PO groups [10], it ensures that the EO and PO beads have comparable sizes of 240 Å^3. Nominal formula and coarse-gained chains of the Pluronic polymers used in this study are listed in Table 1. A small cluster with unit cell crystal structure containing four gold atoms, which may correspond to the primary cluster that was experimentally observed in the early stage of gold nanoparticles formation, is considered as a gold bead. The space group of this crystal is no. 225 with a lattice length of 4.0783 Å [34].

To simulate a system, a set of interacting parameters between beads must be determined. A large value indicates strong repulsive interaction between beads. Groot and Warren [7] established a relationship between DPD repulsive interaction parameters and the well-known Flory–Huggins χ parameter theory for polymer solutions. Maiti and McGrother [37] related the DPD interaction parameters to bead-size, solubility parameter, and surface tension. We take the bead density ρ as 3 and the water–water, EO–EO,

Table 2 Interaction parameters in DPD simulation used in this study

	E	P	W	Au
E	25	48.87	35.93	49.98
P	48.87	25	38.32	26.13
W	35.93	38.32	25	95.42
Au	49.98	26.13	95.42	15

and PO–PO maximum repulsive parameters (a_{ii}) as 25. We then obtain the following relationship for interaction parameters between different components (a_{ij}).

$$a_{ij} = a_{ii} + 3.27\chi_{ij}(\rho = 3) \quad (11)$$

The χ parameters between EO–water, PO–water, and EO–PO have been well estimated from either the correlation of polymer solubility parameters [39] or a simulation method coded as a blend module in Cerius 2 [31]. The blend method, which combines a modified Flory–Huggins model and Monte Carlo simulation to directly calculate the χ parameters from the mixing energy between DPD particles, performed well in DPD simulation lately [20, 25, 31, 34, 39, 40]. On the basis of those χ values, both DPD [31] and Mesodyn [38] simulations allowed describing the aggregation process of PEO–PPO–PEO block copolymers. Thus, we retain those values for this study. However, no consistent protocol has been established to determine the interaction parameters between solid particles and polymers in DPD method. Some recent attempts employed blend method to calculate the interaction parameters between solid particle and polymer fragments [33, 34]. Similarly, we derive the interaction parameters between gold–water, gold–EO, and gold–PO. We set the gold–gold beads to 15, corresponding to strong attractions between gold beads to model the readily aggregation of gold nanoparticles in water. Successful reproductions of the morphologies we see in experiments, as shown in the latter, indicate that the interaction parameters used here are reasonable for the Pluronic–gold–water system. Table 2 gathers the values of all the interaction parameters used in this study.

Simulation size and time The ratio of gold to water is set to 10:100 in all simulations so as to match the one used in the previous experiments [3]. A cubic simulation box with periodic boundary conditions used in each direction was adopted. It is really necessary to test whether the simulation box is large enough to avoid the finite box size effects and the simulation time is long enough to achieve equilibrium, especially in the case of the systems with the long polymer chains. In this paper, we focus on the stabilization of gold nanoparticles by amphiphilic copolymers, which would prevent the nanoparticles from aggregation. Consequently, the size and number of the resulted gold beads clusters are direct and important criteria to value the effects of simulation box size and time. Systems of Pluronic P105, F68, F88, and F108 (5% concentration), which consist of longer coarse-grained chains with 36 up to 83 DPD particles, were simulated in 10×10×10, 15×15×15, 20×20×20, 30×30×30, and 40×40×40 cubic box with 20,000 time steps, respectively. Figure 2 shows the number-average diameters (left axis, solid lines) and total numbers (right axis, dot lines) of the simulated gold nanoparticles in different box sizes. It is found that the average diameter of gold nanoparticles increases with the box size increasing when smaller box was adopted, which may be attributed to the oppression of long-chain polymers by the box boundary. However, the particle sizes are almost the same in 20, 30, and 40 boxes, whereas the number of particles increases in an exponential function of box size. As plotted in Fig. 3, the

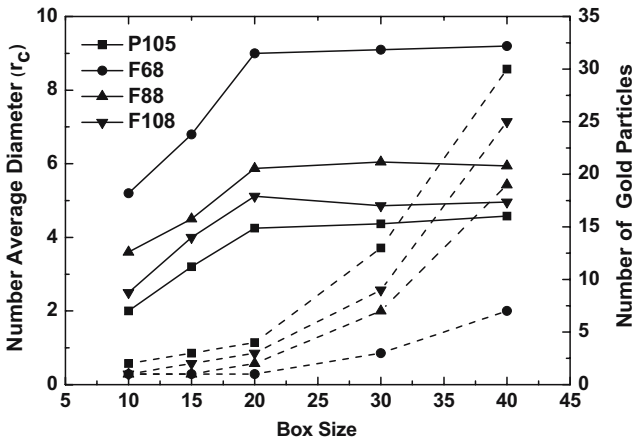

Fig. 2 Number-average diameters (*left axis*, *solid lines*) and total numbers (*right axis*, *dot lines*) of the resulted gold nanoparticles simulated in different box sizes after 20,000 simulation time steps, the copolymer concentration is 5%

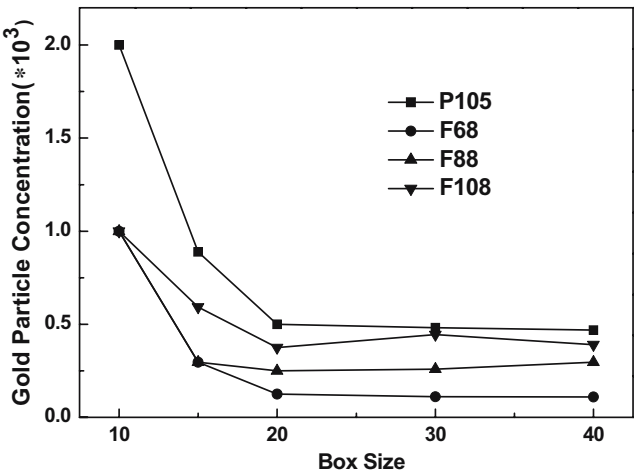

Fig. 3 Concentration of gold nanoparticles simulated in different box sizes after 20,000 simulation time steps, the copolymer concentration is 5%

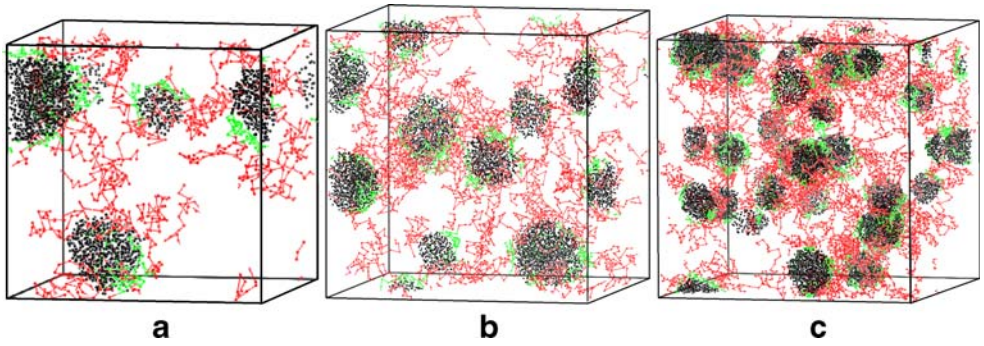

Fig. 4 Simulation results of representative 5% F108 system in 20 (**a**), 30 (**b**), and 40 (**c**) box sizes. The *black*, *green*, and *red portions* represent gold, hydrophobic PO, and hydrophilic EO beads, respectively

concentration of gold particles (number of particles divided by box volume) remains unchanged, while box size is larger than 20. Considering the simulation quality and computation efficiency, a box of 20×20×20 with 20,000 time step runs is indeed sufficient to avoid the finite size effects. Simulation results of a representative F108 system in 20, 30, and 40 boxes are shown in Fig. 4. The black, green, and red portions represent gold, hydrophobic PO, and hydrophilic EO beads, respectively. For the sake of clarity, water is not shown in Fig. 4, neither is for Figs. 7, 9, and 10, 11, 12.

The time dependency of an average diameter of gold particles and the diffusion coefficient of each bead type are monitored to decide the simulation time. Figure 5 presents the time evolution of systems of Pluronic P105, F68, F88, and F108 (5% concentration) in 20×20×20 box. The average particle sizes keep increasing at the initial stage, but retain changeless after 10,000 time steps (t=500) for all systems. The diffusivity of a DPD particle is a dimensionless parameter characterizing the fluid and can be interpreted as the ratio between the time for fluid particles to diffuse a given distance and the time for hydrodynamic

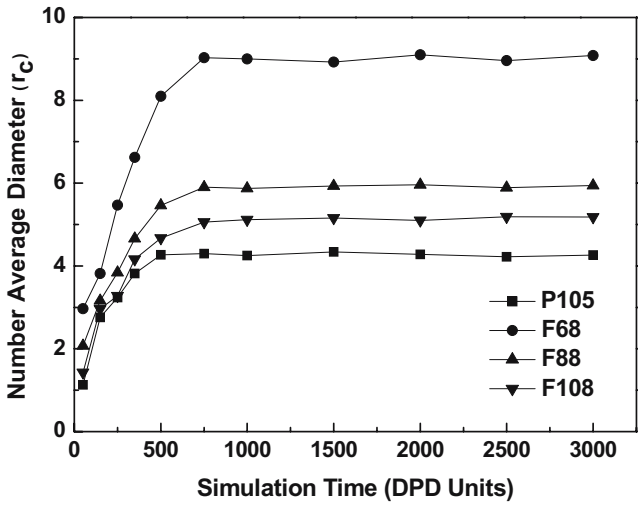

Fig. 5 Evolution of average diameters of the simulated gold nanoparticles as a function of simulation time, box size is 20×20×20, and the copolymer concentration is 5%

interactions to reach steady state on the same distance [7]. Hence, the diffusion coefficient of each bead in DPD simulation could be employed to check the equilibrium of a simulated system [20, 31]. It could be derived by calculating the mean square displacement of each type of bead according to the following equation [10, 41],

$$D = \lim_{t\to\infty} \frac{1}{6t} \left\langle |\vec{r}_i(t) - \vec{r}_i(0)|^2 \right\rangle \tag{12}$$

Figure 6 shows the evolution of the diffusion coefficient of each bead type of a representative F108 system with the simulation time. It is shown that, in the early stage (up to 700 simulation time), the diffusion coefficients of water, gold, and Pluronic are all fluctuant and distinct from each other. This indicates the existence of metastable aggregates. After about 1,000 simulation time, the diffusion coefficient of each type of bead does not change, which indicate the system has already achieved equilibrium. The motion velocities of the EO, PO, and gold become equal but obviously different from that of water. That is to say, the block copolymer and gold assemble together into stable colloids in water. Combining the time evolution of both particle size and diffusion coefficients, it is reasonable that 20,000 time steps (t=1,000) per simulation is indeed sufficient for simulation equilibrium.

Simulation length and time scales The DPD bead interaction range r_c sets the basic length scale of the system and is defined as the side of a cube containing an average number of ρ beads according to Groot et al. [10, 33] Therefore, $r_c=(\rho V_b)^{1/3}$, where V_b is the volume of a bead defined in the simulations. For our parameterization, ρ=3.0 and V_b= 240 Å^3, which implies r_c=0.90 nm and a typical simulation box of 20×20×20 r_c^3 in DPD units, would represent a cube of real spatial dimensions, ~18 nm on each side. Groot and Rabone [10] compared DPD computed diffusion constant of water beads with the experimentally measured values. This analysis led to a DPD time scale given by $\tau \sim 25.7 N_m^{5/3}$ ps for our parameters [42], where N_m is the volume of the bead in terms of water molecules. Considering the partial volume

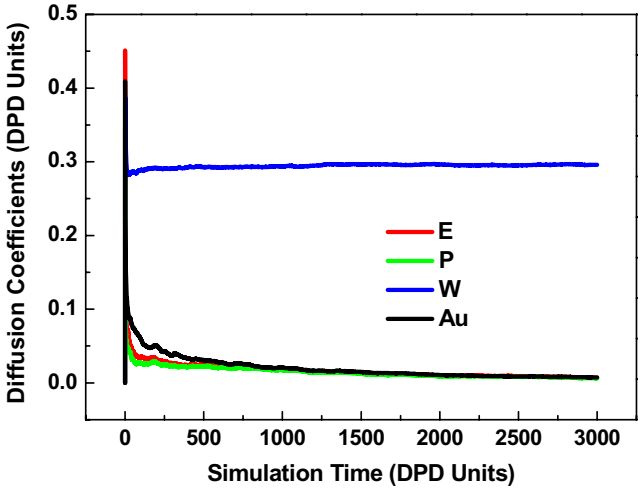

Fig. 6 Evolution of the diffusion coefficient of the DPD beads in 5% F108–gold–water system with the simulation time increasing, box size is 20×20×20

of a water molecule is 30 Å^3, N_m is ~8 in our case, which yields τ~0.82 ns. Therefore, a typical run of 20,000 steps with time step of 0.05τ correspond to a real time of ~0.82 μs.

Results and discussions

Structure and time evolution of Pluronic–gold colloids Figure 7 shows a snapshot of typical simulated Pluronic–gold colloids in 20% P105 aqueous solution system. The black, green, and red portions represent gold, hydrophobic PO, and hydrophilic EO beads, respectively. It is obvious that all Au beads were wrapped by the copolymer and formed spherical particles in the interior part of the Pluronic micelles. The hydrophobic PO segments are adsorbed on the surface of gold particles, whereas the hydrophilic EO ones are in contact with water. Thus Pluronic–gold colloids are of two-layer structures. This confirms the hypothesis of Sakai and Alexandridis [2] that PEO–PPO–PEO block copolymers likely ensure the stabilization of gold nanoparticles through their amphiphilic character and their ability to form micelles on the surface of particles. In the simulated box, there are several spherical gold nanoparticles with almost the same size. Their number-average diameters are calculated to be four DPD units, which correspond to about 3.6 nm in real spatial dimensions according to the length scale in our simulations. The simulated morphology and size of the gold nanoparticles agree well with transmission electron microscope observations in the preceding paper [3].

More detailed information on the structure of gold–copolymer colloids is analyzed by checking lateral bead distributions across the colloids. The simulation box is divided into 80 slices of thickness r_c/4 along to x coordinate, and the numbers of beads of each type were calculated over the thin slices to construct bead density distributions. Average of the densities were taken over the last 1,000 samples of configurations after simulation reached to equilibrium (from 19,000 to 20,000 time steps) [7, 13, 15, 19, 31]. Figure 8 shows the bead density profiles of Pluronic–Au colloids in a 20% P105–gold–water system. The narrow peak of the gold density corresponds to the gold colloidal core. The PO and EO bead density profiles reflect the micelle structure of the PEO–PPO–PEO block copolymer absorbed on the gold surface. As for the water bead, it penetrates the whole aggregates. However, the amount of water decreases from the bulk solution to the colloid core, indicating that the microenvironments inside Pluronic–Au colloids are somewhat hydrophobic.

Knowledge about the formation process is of fundamental importance for controlling the properties of nanomaterials. Figure 9 shows the simulated snapshots of the evolution of Pluronic–gold colloids in aqueous solution as a function of simulation time. In the very early stage up to t=50, gold beads rapidly form small clusters, while the block copolymers tend to aggregate because of their amphiphilic properties. After a period of fluctuation till t=150, some gold clusters were wrapped by the block copolymers once micelles are formed (shown in small circle). They are fairly stable during the subsequent process. However, most gold clusters coalesce and break up in a dynamic manner, forming various metastable structures till micelles are formed on their surfaces (shown in big oval from t=150 to 350). Gold nanoparticles formed in latter time are larger than those formed earlier. It suggested that the formation of Pluronic–gold colloids is controlled by the competition between aggregation of gold clusters and stabilization by micelles of block copolymers. If the latter is much faster

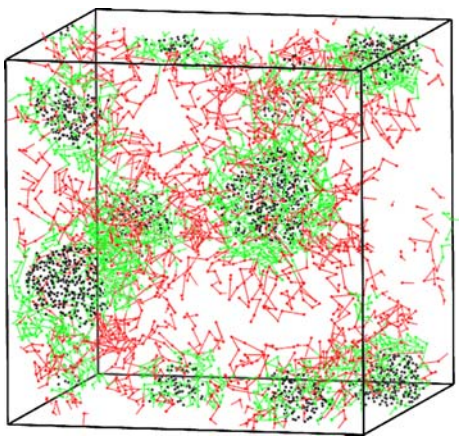

Fig. 7 Snapshot of a representative simulated Pluronic–gold aggregates (20% P105 system) after 1,000 simulation time. The *black*, *green*, and *red portions* represent gold, hydrophobic PO, and hydrophilic EO beads, respectively

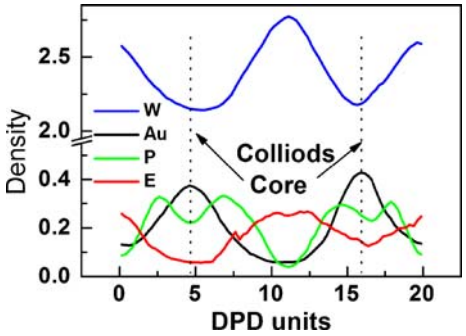

Fig. 8 Bead number density distributions along the *x*-axis according to Pluronic–Au colloids in 20% P105–gold–water system. The simulation box is divided into 80 slices of thickness $r_c/4$ along to *x*-coordinate, and the last 1,000 samples of the number of beads of each type in the slices were used to construct the density profiles. The *blue*, *black*, *green*, and *red line* represents water, gold, P, and E bead, respectively

than the former, small gold clusters formed at the early stage could be wrapped more rapidly by the micelles. Thus, any methods or parameters that promote the micellization of the block copolymers are expected to favor the formation of uniform and small gold nanoparticles. This is consistent with the previous experimental observations that the gold particles are much more uniform and smaller and the Pluronic–gold colloidal systems became much more stable in the presence of salt. That is because the salt added significantly promoted the micellization of the block copolymers [3].

In what follows, the effects of the P105 concentration from 0 to 10%, the molecular weight of the block copolymer (5% F38, F68, F88, and F108 whose EO/PO ratios are the same and whose molecular weights are different), and the PO block length (5% PEO2000, P65, P84, and P123, which have the same EO block length and differ in PO block length) will be simulated to investigate the experimental morphologies obtained in these different conditions.

Effects of Pluronic concentration Figure 10 shows the simulated results of the P105–gold–water system with different P105 concentrations: 0, 1, 5, and 10%. It is presented that without the block copolymer (Fig. 10a), gold beads are unstable and tend to aggregate because of the strong repulsive interactions between gold and water. In the presence of 1% P105 (Fig. 10b), no micelles are formed because of the low P105 concentration; both the PO and EO blocks are absorbed on the surface of gold particles. For 5% P105 system, spherical gold nanoparticles are formed inside the Pluronic micelles. With a further increase in the P105 concentration, particles become even smaller in size and more uniform.

Effects of Pluronic composition Figure 11 presents the simulated results of Pluronic–gold–water system with Pluronics of different molecular weights (5% F38, F68, F88, and F108). These block copolymers all have the same PEO/PPO ratio of 80:20. Their molecular weights increase from F38 to F108. It is shown that, in the cases of F38 and F68, the block copolymers are adsorbed on the surfaces of gold particles. However, they do not form two-layer micelle

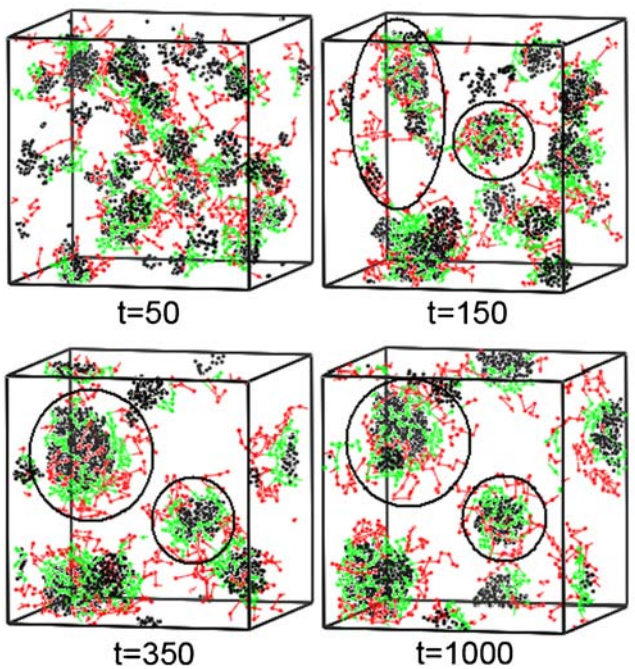

Fig. 9 Snapshots of the evolution of Pluronic–gold colloids in 5% P105 aqueous solution system as a function of simulation time

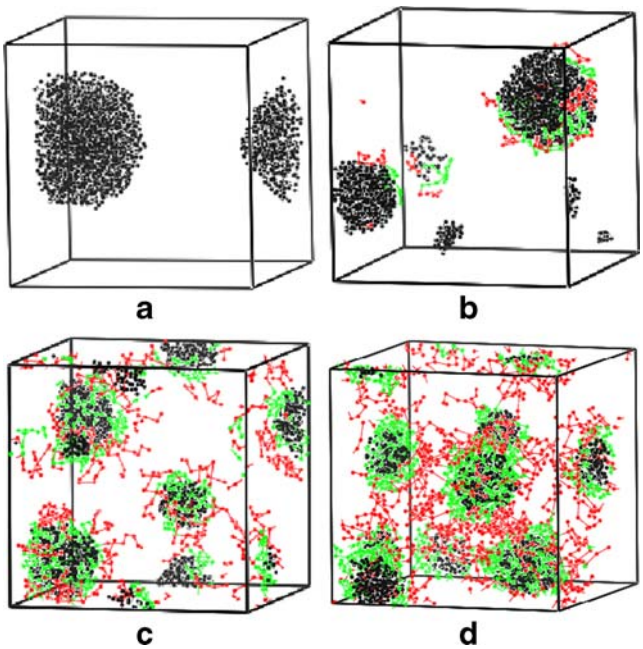

Fig. 10 Simulated morphology of the P105–gold–water system with different P105 concentrations: **a** 0, **b** 1%, **c** 5%, and **d** 10%

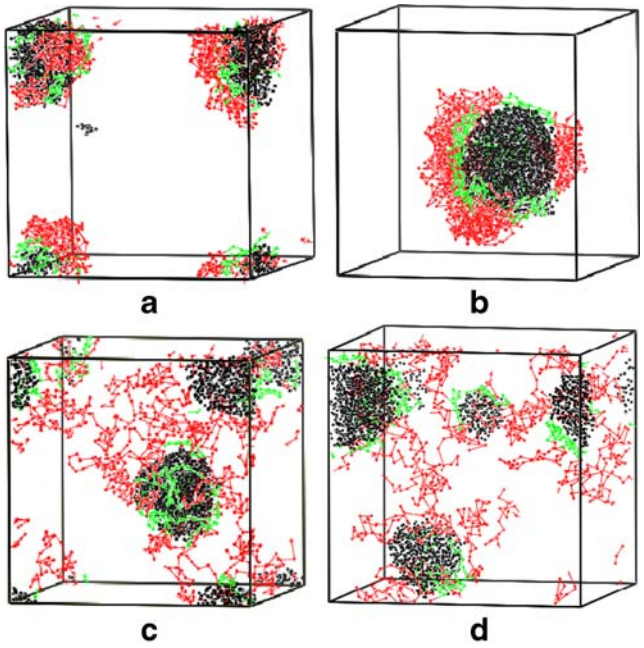

Fig. 11 Simulated morphology of Pluronic–gold–water system with 5% Pluronics of the same PEO/PPO ratio (80:20) and different molecular weights: **a** F38, **b** F68, **c** F88, and **d** F108

structures. Many parts of the surfaces of the gold beads are not wrapped by the block copolymers and are exposed to water. By contrast, in the cases of F88 and F108, gold beads are completely capped inside the block copolymer micelles. This explains why, with these two block copolymers, spherical and uniform gold nanoparticles were experimentally obtained. The reason is that a block copolymer of a higher molecular weight is easier to form micelles as cavities for the formation of gold nanoparticles. Once formed, the latter were better stabilized.

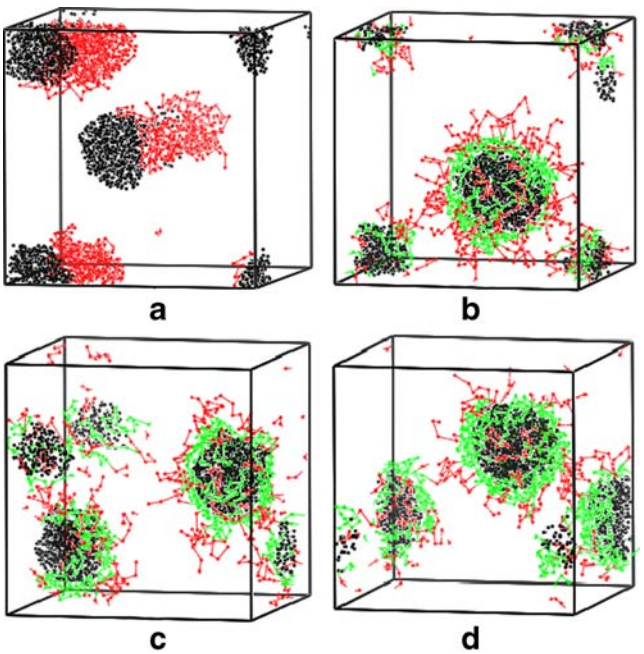

Fig. 12 Simulated morphology of Pluronic–gold–water system with 5% Pluronics of the same PEO block length and different PPO block lengths. **a** PEO2000, **b** P65, **c** P84, and **d** P123

It was reported that PEO–PPO–PEO block copolymers were more efficient than PEO homopolymer as stabilizers of gold nanoparticles because the absorption of PO segments on gold surfaces limited particle growth [2]. The PPO block was a primary factor for the micellization of Pluronic [43]. Thus, we select PEO2000, P65, P84, and P123 to examine the effect of the PPO block length. They all have the same PEO block length (see Table 1). Figure 12 shows the simulated results of these systems with 5% polymer concentration. The PEO homopolymer forms a single hydrophilic and incomplete layer onto the surfaces of the gold particles (Fig. 12a). Therefore, it is unable to prevent gold particles from aggregation. When the PO

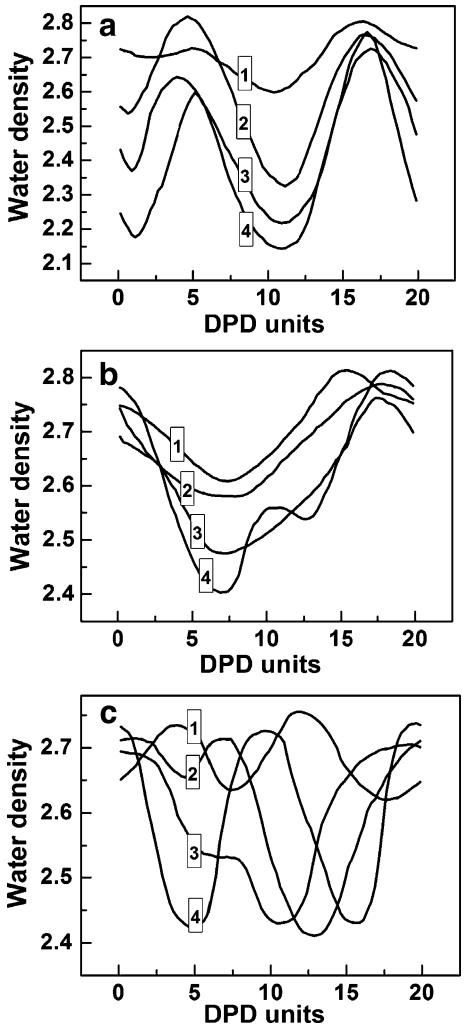

Fig. 13 Simulated water density profiles of various Pluronic–gold–water systems. **a** Various Pluronic concentration: (*1*) 1, (*2*) 5, (*3*) 10, and (*4*) 20% P105; **b** 5% Pluronics with the same PEO/PPO ratio and different molecular weights: (*1*) F38, (*2*) F68, (*3*) F88, and (*4*) F108); **c** 5% Pluronics with the same PEO block length and different PPO block lengths: (*1*) PEO2000, (*2*) P65, (*3*) P84, and (*4*) P123

block is long enough, PEO–PPO–PEO block copolymers form micelles. The latter wrap the gold nanoparticles and prevent them from aggregation (Fig. 12c, d). However, no major difference is found among P64, P85, and P123, likely because their PPO blocks are all long enough.

Water density inside Pluronic–gold colloids In a previous work, we used Fourier transform spectroscopy and ^{1}H NMR to probe the microenvironments inside PEO–PPO–PPO block copolymer micelles [3]. We concluded that a hydrophobic micelle core was favorable for the entrapment of primary gold clusters and stabilization of formed gold nanoparticles. However, we were unable to experimentally measure the water content inside Pluronic–gold colloids. Consequently, we attempt to solve the problem by simulating the density distribution of water beads in Pluronic–gold colloids. Figure 13 shows the water density profiles of the systems simulated above. The minima of each of the curves correspond to the water content inside the Pluronic–gold colloidal cores. It is seen that systems with the highest polymer concentration, highest polymer molecular weight, and/or longest PPO block yield the smallest amount of water inside the colloidal cores. Both experimental and simulation results show that all these systems allow obtaining spherical and uniform gold nanoparticles. Therefore, hydrophobic microenvironments inside micelles favor the stabilization of gold nanoparticles.

Conclusions

DPD simulation was employed to investigate the formation of gold nanoparticles in PEO–PPO–PEO block copolymer micelles. Primary gold clusters observed in the formation of gold nanoparticles were considered as gold beads in DPD simulation. Our simulation successfully reproduced the morphologies and size of gold nanoparticles obtained experimentally, where different Pluronic copolymers were employed as stabilizer. The structure of simulated gold nanoparticles indicated that gold atoms were wrapped by the copolymer and formed spherical particles inside the micelles. The hydrophobic PO segments were adsorbed on the surface of gold particles, whereas the hydrophilic EO segments were exposed to water, forming stable Pluronic–gold colloids with two-layer structures. Density profiles of beads suggested hydrophobic microenvironments inside the colloids. The simulated dynamic process suggested that the morphology and size of gold nanoparticles depended very much on the competition between aggregation of gold clusters and stabilization by micelles of block copolymers.

Increasing Pluronic concentration, its molecular weight, and/or its PPO block length favored the formation and stabilization of spherical and uniform gold nanoparticles. The calculated density distribution of water showed that systems that were efficient in stabilization were all deficient in water content inside the micelle cores, suggesting that hydrophobicity inside the micelles plays a decisive role in the entrapment of primary gold clusters and stabilization of gold nanoparticles. Increasing hydrophobicity inside the copolymer micelles favored the colloidal stabilization and the formation of uniform gold nanoparticles. Our work has demonstrated that DPD methods are effective to study the nanoparticle systems and give useful guidance on the discovery of novel materials.

Acknowledgments This work was financially supported by the National Natural Science Foundation of China (No.20221603, No.20490200, and No. 20676137), the Scientific Research Foundation for the Returned Overseas Chinese Scholars, the Ministry of Education, and the Chinese Academy of Sciences for international cooperation.

References

1. Roucoux A, Schulz J, Patin H (2002) Chem Rev 102:3757
2. Sakai T, Alexandridis P (2004) Langmuir 20:8426
3. Chen S, Guo C, Hu, GH, Wang J, Ma JH, Liang XF, Zheng L, Liu HZ (2006) Langmuir 22:9704
4. Cushing BL, Kolesnichenko VL, O'Connor CJ (2004) Chem Rev 104:3893
5. Burda C, Chen X, Narayanan R, El-Sayed MA (2005) Chem Rev 105:1025
6. Hoogerbrugge PJ, Koelman J (1992) Europhys Lett 19:155
7. Groot RD, Warren PB (1997) J Chem Phys 107:4423
8. Groot RD, Madden TJ (1998) J Chem Phys 108:8713
9. Venturoli M, Smit B (1999) Phys Chem Comm 10:1
10. Groot RD, Rabone KL (2001) Biophys J 81:725
11. Kranenburg M, Venturoli M, Smit B (2003) J Phys Chem B 107:11491
12. Li DW, Liu XY, Feng YP (2004) J Phys Chem B 108:11206
13. Allen MP (2006) J Phys Chem B 110:3823
14. Laradji M, Kumar PBS (2004) Phys Rev Lett 93:198105
15. Shillcock JC, Lipowsky R (2002) J Chem Phys 117:5048
16. Shillcock JC, Lipowsky R (2005) Nat Mater 4:225
17. Yamamoto S, Maruyama Y, Hyodo S (2002) J Chem Phys 116:5842
18. Yamamoto S, Hyodo S (2003) J Chem Phys 118:7937
19. Ortiz V, Nielsen SO, Discher DE, Klein ML, Lipowsky R, Shillcock J (2005) J Phys Chem B 109:17708
20. Yang C, Chen X, Qiu H, Zhuang W, Chai Y, Hao J (2006) J Phys Chem B 110:21735
21. Rekvig L, Hafskjold B, Smit B (2004) Langmuir 20:11583
22. Qian HJ, Lu ZY, Chen LJ, Li ZS, Sun CC (2005) Macromolecules 38:1395
23. Jury S, Bladon P, Cates M, Krishna S, Hagen M, Ruddock N, Warren P (1999) Phys Chem Chem Phys 1:2051
24. Schulz SG, Kuhn H, Schmid G, Mund C, Venzmer J (2004) Colloid Polym Sci 283:284
25. Yuan SL, Cai ZT, Xu GY, Jiang YS (2002) Chem Phys Lett 365:347
26. Nakamura H (2004) Mol Simulat 30:941
27. Gibson JB, Chen K, Chynoweth S (1998) J Colloid Interf Sci 206:464

28. Malfreyt P, Tildesley DJ (2000) Langmuir 16:4732
29. Clark AT, Lal M, Ruddock JN, Warren PB (2000) Langmuir 16:6342
30. Kong B, Yang X (2006) Langmuir 22:2065
31. Cao X, Xu G, Li Y, Zhang Z (2005) J Phys Chem A 109:10418
32. Laradji M, Hore MJA (2004) J Chem Phys 121:10641
33. Maiti A, Wescott J, Kung P (2005) Mol Simulat 31:143
34. Juan SCC, Hua CY, Chen CL, Sun X, Xi H (2005) Mol Simulat 31:277
35. van Vlimmeren BAC, Maurits NM, Zvelindovsky AV, Sevink GJA, Fraaije JGEM (1999) Macromolecules 32:646
36. Guo SL, Hou TJ, Xu XJ (2002) J Phys Chem B 106:11397
37. Maiti A, McGrother S (2004) J Chem Phys 120:1594
38. Lam YM, Goldbeck-Wood G, Boothroyd C (2004) Mol Simulat 30:239
39. Li YM, Xu GY, Luan YX, Yuan SL, Zhang ZQ (2005) Colloid Surf A 385:257
40. Yuan SL, Cai ZT, Xu GY, Jiang YS (2003) Colloid Polym Sci 281:1069
41. Wu H, Xu J, He X, Zhao Y, Wen H (2006) Colloid Surf A 290:239
42. Groot RD (2003) J Chem Phys 118:11265
43. Guo C, Liu HZ, Chen JY (1999) Colloid Polym Sci 277:376